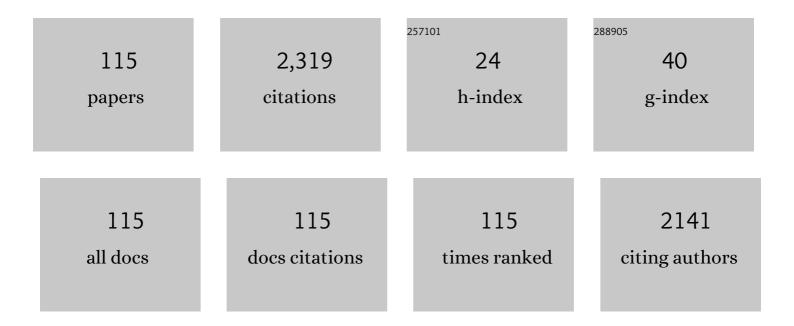
Jakapan Chantana

List of Publications by Year in descending order

Source: https://exaly.com/author-pdf/5129702/publications.pdf Version: 2024-02-01



#	Article	IF	CITATIONS
1	A review of Sb2Se3 photovoltaic absorber materials and thin-film solar cells. Solar Energy, 2020, 201, 227-246.	2.9	243
2	Highly Efficient 17.6% Tin–Lead Mixed Perovskite Solar Cells Realized through Spike Structure. Nano Letters, 2018, 18, 3600-3607.	4.5	114
3	Impact of Urbach energy on open-circuit voltage deficit of thin-film solar cells. Solar Energy Materials and Solar Cells, 2020, 210, 110502.	3.0	107
4	Impact of growth temperature on the properties of SnS film prepared by thermal evaporation and its photovoltaic performance. Current Applied Physics, 2015, 15, 897-901.	1.1	98
5	Theoretical analysis of band alignment at back junction in Sn–Ge perovskite solar cells with inverted p-i-n structure. Solar Energy Materials and Solar Cells, 2020, 206, 110268.	3.0	66
6	Structural and Solar Cell Properties of a Ag-Containing Cu ₂ ZnSnS ₄ Thin Film Derived from Spray Pyrolysis. ACS Applied Materials & Interfaces, 2018, 10, 5455-5463.	4.0	61
7	Introduction of Na into Cu 2 SnS 3 thin film for improvement of its photovoltaic performances. Solar Energy Materials and Solar Cells, 2017, 168, 207-213.	3.0	49
8	Investigation of carrier recombination of Na-doped Cu2SnS3 solar cell for its improved conversion efficiency of 5.1%. Solar Energy Materials and Solar Cells, 2020, 206, 110261.	3.0	46
9	Thin-film Cu(In,Ga)(Se,S) ₂ -based solar cell with (Cd,Zn)S buffer layer and Zn _{1â^²<i>x</i>} Mg _{<i>x</i>} O window layer. Progress in Photovoltaics: Research and Applications, 2017, 25, 431-440.	4.4	41
10	Aluminumâ€doped Zn _{1Ââ^'Â<i>x</i>} Mg _{<i>x</i>} O as transparent conductive oxide of Cu(In,Ga)(S,Se) ₂ â€based solar cell for minimizing surface carrier recombination. Progress in Photovoltaics: Research and Applications, 2017, 25, 996-1004.	4.4	39
11	20% Efficient Zn _{0.9} Mg _{0.1} O:Al/Zn _{0.8} Mg _{0.2} O/Cu(In,Ga)(S,Se) _{2Solar Cell Prepared by All-Dry Process through a Combination of Heat-Light-Soaking and Light-Soaking Processes. ACS Applied Materials & amp; Interfaces, 2018, 10, 11361-11368.}	^{>} 4.0	38
12	Flexible Cu(In,Ga)Se ₂ solar cell on stainless steel substrate deposited by multiâ€layer precursor method: its photovoltaic performance and deepâ€level defects. Progress in Photovoltaics: Research and Applications, 2016, 24, 990-1000.	4.4	35
13	Optimum bandgap profile analysis of Cu(In,Ga)Se ₂ solar cells with various defect densities by SCAPS. Japanese Journal of Applied Physics, 2014, 53, 04ER14.	0.8	33
14	Impact of annealing treatment before buffer layer deposition on Cu 2 ZnSn(S,Se) 4 solar cells. Thin Solid Films, 2015, 582, 151-153.	0.8	33
15	Investigation of Cu(In,Ga)Se 2 absorber by time-resolved photoluminescence for improvement of its photovoltaic performance. Solar Energy Materials and Solar Cells, 2014, 130, 567-572.	3.0	32
16	Uniqueness verification of direct solar spectral index for estimating outdoor performance of concentrator photovoltaic systems. Renewable Energy, 2015, 75, 762-766.	4.3	32
17	Investigation of correlation between open-circuit voltage deficit and carrier recombination rates in Cu(In,Ga)(S,Se)2-based thin-film solar cells. Applied Physics Letters, 2018, 112, 151601.	1.5	32
18	Numerical reproduction of a perovskite solar cell by device simulation considering band gap grading. Optical Materials, 2019, 92, 60-66.	1.7	32

Jakapan Chantana

#	Article	IF	CITATIONS
19	Investigation on evaporation and suppression of SnS during fabrication of Cu ₂ SnS ₃ thin films. Physica Status Solidi (A) Applications and Materials Science, 2015, 212, 2289-2296.	0.8	31
20	Impact of Precursor Compositions on the Structural and Photovoltaic Properties of Sprayâ€Deposited Cu ₂ ZnSnS ₄ Thin Films. ChemSusChem, 2016, 9, 2414-2420.	3.6	31
21	Heterointerface recombination of Cu(In,Ca)(S,Se) ₂ â€based solar cells with different buffer layers. Progress in Photovoltaics: Research and Applications, 2018, 26, 127-134.	4.4	31
22	Na role during sulfurization of NaF/Cu/SnS 2 stacked precursor for formation of Cu 2 SnS 3 thin film as absorber of solar cell. Applied Surface Science, 2017, 414, 140-146.	3.1	29
23	Colorful, Flexible, and Lightweight Cu(In,Ga)Se ₂ Solar Cell by Lift-Off Process With Automotive Painting. IEEE Journal of Photovoltaics, 2018, 8, 1326-1330.	1.5	27
24	Impact of Auger recombination on performance limitation of perovskite solar cell. Solar Energy, 2021, 217, 342-353.	2.9	27
25	Enhancement of photovoltaic performances of Cu (In,Ga)(S,Se) ₂ solar cell through combination of heatâ€light soaking and light soaking processes. Progress in Photovoltaics: Research and Applications, 2018, 26, 868-876.	4.4	26
26	Aging Effect of a Cu(In,Ga)(S,Se) 2 Absorber on the Photovoltaic Performance of Its Cdâ€Free Solar Cell Fabricated by an Allâ€Dry Process: Its Carrier Recombination Analysis. Advanced Energy Materials, 2019, 9, 1902869.	10.2	26
27	Sputtered (Zn,Mg)O buffer layer for band offset control in Cu ₂ ZnSn(S,Se) ₄ solar cells. Japanese Journal of Applied Physics, 2014, 53, 106502.	0.8	24
28	Characteristics of Zn1â^'xMgxO:B and its application as transparent conductive oxide layer in Cu(In,Ga)(S,Se)2 solar cells with and without CdS buffer layer. Solar Energy, 2019, 184, 553-560.	2.9	24
29	Influence of conduction band minimum difference between transparent conductive oxide and absorber on photovoltaic performance of thin-film solar cell. Japanese Journal of Applied Physics, 2015, 54, 032301.	0.8	23
30	Influence of Na in Cu2SnS3 film on its physical properties and photovoltaic performances. Thin Solid Films, 2017, 636, 431-437.	0.8	23
31	Influences of environmental factors on Si-based photovoltaic modules after longtime outdoor exposure by multiple regression analysis. Renewable Energy, 2017, 101, 10-15.	4.3	23
32	Examination of Relationship between Urbach Energy and Open-Circuit Voltage Deficit of Flexible Cu(In,Ga)Se2 Solar Cell for Its Improved Photovoltaic Performance. ACS Applied Energy Materials, 2019, 2, 7843-7849.	2.5	22
33	Controlled back slope of Ga/(In+Ga) profile in Cu(In,Ga)Se2 absorber fabricated by multi layer precursor method for improvement of its photovoltaic performance. Solar Energy Materials and Solar Cells, 2015, 133, 223-228.	3.0	21
34	Physical and chemical aspects at the interface and in the bulk of CuInSe ₂ -based thin-film photovoltaics. Physical Chemistry Chemical Physics, 2022, 24, 1262-1285.	1.3	21
35	Trap-assisted recombination for ohmic-like contact at p-type Cu(In,Ga)Se2/back n-type TCO interface in superstrate-type solar cell. Journal of Applied Physics, 2016, 120, .	1.1	20
36	Spectral mismatch correction factor indicated by average photon energy for precise outdoor performance measurements of different-type photovoltaic modules. Renewable Energy, 2017, 114, 567-573.	4.3	19

#	Article	IF	CITATIONS
37	Application of Al-Doped (Zn, Mg)O on pure-sulfide Cu(In, Ga)S2 solar cells for enhancement of open-circuit voltage. Solar Energy Materials and Solar Cells, 2019, 202, 110157.	3.0	19
38	Impact of average photon energy on spectral gain and loss of various-type PV technologies at different locations. Renewable Energy, 2020, 145, 1317-1324.	4.3	19
39	Localized surface plasmon enhanced microcrystalline–silicon solar cells. Journal of Non-Crystalline Solids, 2012, 358, 2319-2323.	1.5	18
40	Application of multi-buffer layer of (Zn,Mg)O/CdS in Cu2ZnSn(S,Se)4 solar cells. Current Applied Physics, 2015, 15, 383-388.	1.1	18
41	ZnSnP2 solar cell with (Cd,Zn)S buffer layer: Analysis of recombination rates. Solar Energy Materials and Solar Cells, 2018, 174, 412-417.	3.0	18
42	Characterization of Cd-Free Zn _{1–<i>x</i>} Mg _{<i>x</i>} O:Al/Zn _{1–<i>x</i>} Mg _{<i>x</i>} O Solar Cells Fabricated by an All Dry Process Using Ultraviolet Light Excited Time-Resolved Photoluminescence. ACS Applied Materials & amp; Interfaces, 2019, 11, 7539-7545.	D/Cu(In,Ga 4.0)(S.Se)
43	Back-contact barrier analysis to develop flexible and bifacial Cu(In,Ca)Se2 solar cells using transparent conductive In2O3: SnO2 thin films. Solar Energy, 2020, 211, 1311-1317.	2.9	18
44	Determination of open-circuit voltage in Cu(In,Ga)Se2solar cell by averaged Ga/(In + Ga) near its absorber surface. Journal of Applied Physics, 2013, 114, 084501.	1.1	17
45	Description of degradation of output performance for photovoltaic modules by multiple regression analysis based on environmental factors. Optik, 2019, 179, 1063-1070.	1.4	17
46	22%â€efficient Cdâ€free Cu(In,Ga)(S,Se) ₂ solar cell by allâ€dry process using Zn _{0.8} Mg _{0.2} O and Zn _{0.9} Mg _{0.1} O:B as buffer and transparent conductive oxide layers. Progress in Photovoltaics: Research and Applications, 2020, 28, 79-89.	4.4	17
47	Superstrate-type flexible and bifacial Cu(In,Ga)Se2 thin-film solar cells with In2O3:SnO2 back contact. Solar Energy, 2020, 211, 725-731.	2.9	17
48	Application of Two-Dimensional MoSe2 Atomic Layers to the Lift-Off Process for Producing Light-Weight and Flexible Bifacial Cu(In, Ga)Se2 Solar Cells. ACS Applied Energy Materials, 2020, 3, 9504-9508.	2.5	17
49	Transparent Electrode and Buffer Layer Combination for Reducing Carrier Recombination and Optical Loss Realizing over a 22%-Efficient Cd-Free Alkaline-Treated Cu(In,Ga)(S,Se)2 Solar Cell by the All-Dry Process. ACS Applied Materials & Interfaces, 2020, 12, 22298-22307.	4.0	17
50	Impact of Ga/(In + Ga) profile in Cu(In,Ga)Se2 prepared by multi-layer precursor method on its cell performance. Thin Solid Films, 2014, 556, 499-502.	0.8	16
51	Solar cells using bulk crystals of rare metal-free compound semiconductor ZnSnP ₂ . Physica Status Solidi (A) Applications and Materials Science, 2017, 214, 1600650.	0.8	15
52	Influence of halogen content in mixed halide perovskite solar cells on cell performances through device simulation. Solar Energy Materials and Solar Cells, 2020, 205, 110252.	3.0	15
53	Time-resolved photoluminescence of Cu(In,Ga)(Se,S) 2 thin films and temperature dependent current density-voltage characteristics of their solar cells on surface treatment effect. Current Applied Physics, 2017, 17, 461-466.	1.1	14
54	Fabrication of flexible and bifacial Cu(In,Ca)Se2 solar cell with superstrate-type structure using a lift-off process. Solar Energy, 2020, 199, 819-825.	2.9	14

4

Jakapan Chantana

#	Article	IF	CITATIONS
55	Physical properties of Cu(In,Ga)Se2 film on flexible stainless steel substrate for solar cell application: A multi-layer precursor method. Solar Energy Materials and Solar Cells, 2015, 143, 510-516.	3.0	13
56	Impact of Heterointerfaces in Solar Cells Using ZnSnP ₂ Bulk Crystals. ACS Applied Materials & Interfaces, 2017, 9, 33827-33832.	4.0	13
57	Flexible Cu(In,Ga)Se2 solar cell with superstrate-type configuration fabricated by a lift-off process. Thin Solid Films, 2018, 662, 110-115.	0.8	13
58	Development of flexible Cd-free Cu(In,Ga)Se2 solar cell on stainless steel substrate through multi-layer precursor method. Journal of Alloys and Compounds, 2018, 756, 111-116.	2.8	13
59	Structures of Cu(In,Ga)(S,Se) ₂ solar cells for minimizing openâ€circuit voltage deficit: Investigation of carrier recombination rates. Progress in Photovoltaics: Research and Applications, 2019, 27, 630-639.	4.4	13
60	Description of performance degradation of photovoltaic modules using spectral mismatch correction factor under different irradiance levels. Renewable Energy, 2019, 141, 444-450.	4.3	13
61	Mobility improvement of Zn1-xMgxO:Al prepared under room temperature by co-sputtering through optimizations of Al and Mg contents. Materials Science in Semiconductor Processing, 2020, 109, 104921.	1.9	13
62	Device design for high-performance bifacial Cu(In,Ga)Se2 solar cells under front and rear illuminations. Solar Energy, 2021, 218, 76-84.	2.9	13
63	Annealing effect on Cu ₂ ZnSn(S,Se) ₄ solar cell with Zn _{1–<i>x</i>} Mg <i>_x</i> O buffer layer. Physica Status Solidi (A) Applications and Materials Science, 2015, 212, 2766-2771.	0.8	12
64	Influence of minimum position in [Ga]/([Ga]+[In]) profile of Cu(In,Ga)Se2 on flexible stainless steel substrate on its photovoltaic performances. Solar Energy Materials and Solar Cells, 2016, 157, 750-756.	3.0	12
65	ZnSnP 2 thin-film solar cell prepared by phosphidation method under optimized Zn/Sn atomic ratio of its absorbing layer. Current Applied Physics, 2017, 17, 557-564.	1.1	12
66	Urbach energy of Cu(In,Ga)Se2 and Cu(In,Ga)(S,Se)2 absorbers prepared by various methods: Indicator of their quality. Materials Today Communications, 2019, 21, 100652.	0.9	12
67	Effect of Alkali Treatment on Photovoltaic Performances of Cu(In,Ga)(S,Se) ₂ Solar Cells and Their Absorber Quality Analyzed by Urbach Energy and Carrier Recombination Rates. ACS Applied Energy Materials, 2020, 3, 1292-1297.	2.5	12
68	Optimized bandgaps of top and bottom subcells for bifacial two-terminal tandem solar cells under different back irradiances. Solar Energy, 2021, 220, 163-174.	2.9	12
69	Influence of Cu/(Ge + Sn) composition ratio on photovoltaic performances of Cu 2 Sn 1â^'x Ge x S 3 solar cell. Solar Energy, 2017, 149, 341-346.	2.9	11
70	Gasâ€ŧemperature control in VHF―PECVD process for highâ€rate (>5 nm/s) growth of microcrystalline silicon thin films. Physica Status Solidi C: Current Topics in Solid State Physics, 2010, 7, 521-524.	0.8	10
71	Relationship between open-circuit voltage in Cu(In,Ga)Se2 solar cell and peak position of (220/204) preferred orientation near its absorber surface. Applied Physics Letters, 2013, 103, .	1.5	10
72	Ohmic-like contact formation at the rear interface between Cu(In,Ga)Se2 and ZnO:Al in a lift-off Cu(In,Ga)Se2 solar cell. Thin Solid Films, 2016, 616, 17-22.	0.8	10

#	Article	IF	CITATIONS
73	Examination of electrical and optical properties of Zn1â^'xMgxO:Al fabricated by radio frequency magnetron co-sputtering. Thin Solid Films, 2018, 646, 105-111.	0.8	10
74	Influences of Fe and absorber thickness on photovoltaic performances of flexible Cu(In,Ga)Se2 solar cell on stainless steel substrate. Solar Energy, 2018, 173, 126-131.	2.9	10
75	Thermodynamic limit of tandem solar cells under different solar spectra and their perovskite top solar cell. Optical Materials, 2021, 113, 110819.	1.7	10
76	Spectral mismatch correction factor for precise outdoor performance evaluation and description of performance degradation of different-type photovoltaic modules. Solar Energy, 2019, 181, 169-177.	2.9	9
77	Description of short circuit current of outdoor photovoltaic modules by multiple regression analysis under various solar irradiance levels. Renewable Energy, 2020, 147, 895-902.	4.3	9
78	Influence of Ge/(Ge+Sn) composition ratio in Cu2Sn1-xGexS3 thin-film solar cells on their physical properties and photovoltaic performances. Solar Energy Materials and Solar Cells, 2020, 208, 110382.	3.0	9
79	Bismuthâ€doped Cu(In,Ca)Se ₂ absorber prepared by multiâ€layer precursor method and its solar cell. Physica Status Solidi C: Current Topics in Solid State Physics, 2015, 12, 680-683.	0.8	8
80	Estimation of open-circuit voltage of Cu(In,Ga)Se2 solar cells before cell fabrication. Renewable Energy, 2015, 76, 575-581.	4.3	8
81	Interfacial modification mechanism by aging effect for high-performance Cd-free and all-dry process Cu(In,Ga)(S,Se)2 solar cells. Applied Physics Letters, 2020, 117, .	1.5	8
82	Spectral gain and loss of different-type photovoltaic modules through average photon energy of various locations in Japan. Solar Energy, 2021, 214, 1-10.	2.9	8
83	Evaluation of junction quality of buffer-free Zn(O,S):Al/Cu(In,Ga)Se ₂ thin-film solar cells. Applied Physics Express, 2014, 7, 125503.	1.1	7
84	Multi layer precursor method for Cu(In,Ga)Se ₂ solar cells fabricated on flexible substrates. Japanese Journal of Applied Physics, 2014, 53, 05FW03.	0.8	7
85	Evaluation of sputtering damage in Cu ₂ ZnSn(S,Se) ₄ solar cells with CdS and (Cd,Zn)S buffer layers by photoluminescence measurement. Japanese Journal of Applied Physics, 2015, 54, 042302.	0.8	7
86	Effects of Na and secondary phases on physical properties of SnS thin film after sulfurization process. Japanese Journal of Applied Physics, 2016, 55, 092301.	0.8	7
87	Manipulation of [Ga]/([Ga]Â+Â[In]) profile in 1.4-μm-thick Cu(In,Ga)Se2 thin film on flexible stainless steel substrate for enhancing short-circuit current density and conversion efficiency of its solar cell. Solar Energy, 2020, 204, 231-237.	2.9	7
88	Silver-alloyed wide-gap CuGaSe2 solar cells. Solar Energy, 2021, 230, 509-514.	2.9	7
89	Bismuth-doped Cu(In,Ga)Se2 solar cell on flexible stainless steel substrate: Examination of bismuth-doping effectiveness under different substrate temperatures on photovoltaic performances. Solar Energy, 2020, 208, 20-30.	2.9	6
90	Formation of Native In _{<i>x</i>} (O,S) _{<i>y</i>} Buffer through Surface Oxidation of Cu(In,Ga)(S,Se) ₂ Absorber for Significantly Enhanced Conversion Efficiency of Flexible and Cdâ€Free Solar Cell by Allâ€Dry Process. Solar Rrl, 2022, 6, .	3.1	6

#	Article	IF	CITATIONS
91	Effect of thermal annealing and hydrogen-plasma treatment in boron-doped microcrystalline silicon. Journal of Non-Crystalline Solids, 2012, 358, 1966-1969.	1.5	5
92	Effect of crystal orientation in Cu(In,Ga)Se 2 fabricated by multi-layer precursor method on its cell performance. Applied Surface Science, 2014, 314, 845-849.	3.1	5
93	Raman scattering peak position of Cu(In,Ga)Se2 film to predict its near-surface [Ga] / ([Ga] + [In]) and open-circuit voltage. Thin Solid Films, 2015, 582, 7-10.	0.8	5
94	Micro-scale current path distributions of Zn1-Mg O-coated SnO2:F transparent electrodes prepared by sol-gel and sputtering methods in perovskite solar cells. Thin Solid Films, 2019, 669, 455-460.	0.8	5
95	Mg Content Impact of a Sputtered Zn _{1–<i>x</i>} Mg _{<i>x</i>} O:Al Transparent Electrode on Photovoltaic Performances of Flexible, Cd-Free, and All-Dry-Process Cu(In,Ga)(S,Se) ₂ Solar Cells. ACS Applied Energy Materials, 2022, 5, 2270-2278.	2.5	5
96	Derived Conduction Band Offset by Photoelectron Yield Spectroscopy and Its Quantitative Number for Efficiency Enhancement of Flexible, Cd-Free, and All-Dry Process Zn _{1–<i>x</i>} Mg _{<i>x</i>} O:Al/Zn _{1–<i>x</i>} Mg _{<i>x</i>} C Solar Cells. ACS Applied Electronic Materials, 2022, 4, 2077-2085.)/Cu(ln,Ga)(ີ່ຮຸ,Se)
97	Numerical analysis of Cu(In,Ga)Se ₂ solar cells with high defect density layer at back side of absorber. Physica Status Solidi C: Current Topics in Solid State Physics, 2015, 12, 638-642.	0.8	4
98	Utilization of spectral mismatch correction factor for estimation of precise outdoor performance under different average photon energies. Renewable Energy, 2020, 157, 173-181.	4.3	4
99	Effect of an Ohmic back contact on the stability of Cu(In,Ga)Se2-based flexible bifacial solar cells. Applied Physics Letters, 2021, 119, .	1.5	4
100	Zn1â^'xMgxO second buffer layer of Cu2Sn1â^'xGexS3 thin-film solar cell for minimizing carrier recombination and open-circuit voltage deficit. Solar Energy, 2020, 204, 769-776.	2.9	4
101	Gaussian distribution of average photon energy and spectral gain and loss of several-type photovoltaic modules at different outdoor sites around the world. Optics Communications, 2022, 505, 127516.	1.0	4
102	[Ga]/([Ga]+[In]) profile controlled through Ga flux for performance improvement of Cu(In,Ga)Se2 solar cells on flexible stainless steel substrates. Journal of Alloys and Compounds, 2022, 899, 163276.	2.8	4
103	Importance of Starting Procedure for Film Growth in Substrate-Type Microcrystalline-Silicon Solar Cells. Japanese Journal of Applied Physics, 2011, 50, 045806.	0.8	3
104	Investigation of near-surface material composition of Cu(In,Ga)Se ₂ film after air exposure and chemical etching for its Cd-free solar cell. Japanese Journal of Applied Physics, 2018, 57, 121201.	0.8	3
105	Accurate estimation of outdoor performance of photovoltaic module through spectral mismatch correction factor under wide range of solar spectrum. Current Applied Physics, 2021, 28, 59-71.	1.1	3
106	Theoretical impacts of single band gap grading of perovskite and valence band offset of perovskite/hole transport layer interface on its solar cell performances. Solar Energy, 2022, 231, 684-693.	2.9	3
107	The relationship between \$I_{{m H}_{m alpha } } /(I_{{m SiH}}^*)^2\$ and crystalline volume fraction in microcrystalline silicon growth. Physica Status Solidi (A) Applications and Materials Science, 2010, 207, 587-590.	0.8	2
108	Post annealing effect on buffer-free CuInS2solar cells with transparent conducting Zn1â^'xMgxO:Al films. Japanese Journal of Applied Physics, 2014, 53, 05FW04.	0.8	2

#	Article	IF	CITATIONS
109	Highly Decorative, Lightweight Flexible Solar Cells for Automotive Applications. , 0, , .		2
110	Effect of ammonia etching on structural and electrical properties of Cu2ZnSn(S,Se)4 absorbers. Applied Surface Science, 2015, 353, 209-213.	3.1	1
111	Tunableâ€Conductionâ€Band Inâ^'Znâ^'Oâ€based Transparent Conductive Oxide Deposited at Room Temperature Physica Status Solidi (A) Applications and Materials Science, 0, , .	·0.8	1
112	Estimation of annual energy generation of perovskite/crystalline Si tandem solar cells with different configurations in central part of Japan. Renewable Energy, 2022, 195, 896-905.	4.3	1
113	Position Influence of Sputtered Zn _{1â€"<i>x</i>} Mg <i>_x</i> O/Zn _{1â€"<i>x</i>} Mg <i>_x</i>	4.0	1
114	Influence of hetero-interfaces on photovoltaic performance in solar cells based on ZnSnP2 bulk crystal. , 2017, , .		0
115	Peeling Technique by Two-Dimensional MoSe2 Atomic Layer for Bifacial-Flexible Cu(In, Ga)Se2 solar cells. , 2021, , .		0